Chemical Engineering Journal 150 (2009) 252–260

Contents lists available at ScienceDirect

Chemical Engineering Journal

journal homepage: www.elsevier.com/locate/cej

Numerical algorithm for modeling of reactive separation column with fast chemical reaction

Juraj Sláva, Ľudovít Jelemenský, Jozef Markoš*

Institute of Chemical and Environmental Engineering, Faculty of Chemical and Food Technology, Slovak University of Technology, Radlinského 9, 812 37 Bratislava, Slovak Republic

ARTICLE INFO

Article history:
Received 10 December 2008
Received in revised form 2 March 2009
Accepted 3 March 2009

Keywords:
Reactive distillation
Film model
Non-equilibrium model
Fast reaction
Adaptive grid

ABSTRACT

The goal of this paper was to create a non-equilibrium model of a reactive distillation column with very fast homogeneous reaction in the liquid phase. When very fast homogeneous reactions proceed in the liquid film and in the bulk liquid phase, a reaction—diffusion model based on the Fick's equation can be used. Within each iteration of the bulk MESH equations solution, the boundary value problem (reaction and diffusion in the liquid film) had to be solved using automatically adjusted discretization grid for the spatial derivatives discretization. The algorithm proved to be a robust tool for modeling both reactive distillation and absorption, mainly in case of the column performance optimization or in safety analysis, when numerical stability of the solution and algorithm robustness are required not to fail when the column parameters and performance conditions are changed in a wide range.

1. Introduction

The combination of a distillation unit with chemical reaction (reactive distillation, RD) brings several benefits such as a decrease in capital investments and energetic demands, reduction of the catalyst amount, increase of conversion and decrease of side product formation, etc. In the last two decades, the amount of RD units built and run industrially has significantly increased, mainly for processes like esterification, etherification, and alkylation [1]. However, integration of reaction and separation into one unit brings also several problems in the design of the unit scale and optimal operational conditions.

European directive 96/82/EC and related national acts of EU countries on the control of major industrial accidents require a detailed safety analysis of all designed and projected industrial units. In case that projectors and designers have just projected a similar unit of the same size and production capacity and have strong feedback from its industrial installation and performance, such analysis can be done using a comparative method using practical experience and data. In case of a brand-new unit, appropriate mathematical model is a useful tool for such analysis [2,3], usually linked with some methodology commonly used for safety analysis (e.g. HAZOP, [4–7]). The mathematical model used for the description of unit behavior must:

- simulate behavior of the analyzed unit in different regimes of its performance as precisely as possible,
- all parameters needed for the model should be estimated from an independent experiment (kinetic parameters) or empirical or semi empirical correlations (mass-transfer coefficients),
- include a robust algorithm for model equations (usually system of strongly non-linear differential and algebraic equations) solution which cannot fail even if higher deviations from the normal operation point are generated.

The latter is the goal of this paper.

To develop an exact mathematical model able to describe all important phenomena occurring in an RD unit (reaction equilibrium, reaction kinetics, multicomponent phase equilibria, multicomponent mass and heat transfer, etc.) and their cross interactions connected with unit hardware (scale, construction details, packing, vapor and liquid distribution along the unit, etc.) is almost impossible. Two main approaches can be used in the mathematical model development. Equilibrium models assume thermodynamic equilibrium between liquid and vapor leaving the RD column's tray. Non-equilibrium models involving the film theory assume that phase equilibrium occurs only on the vapor–liquid interface. Mass and heat transfer resistance is then located predominantly in the thin films on both sides of the interface. Several different mod-

Abbreviations: BC, boundary condition; BVP, boundary value problem; CSTR, continuous stirred tank reactor; EQ, equilibrium; HAZOP, HAZard and OPerability study; IMSL, International Mathematics and Statistics Library; MESH, Material balance, Equilibrium, Summation and entHalpy balance equations; MS, Maxwell–Stefan approach; NAE, non-linear algebraic equations; NEQ, non-equilibrium; ODE, ordinary differential equations; RD, reactive distillation.

* Corresponding author. Tel.: +421 2 59325 259.
E-mail address: jozef.markos@stuba.sk (J. Markoš).

1385-8947/$ – see front matter © 2009 Elsevier B.V. All rights reserved.
doi:10.1016/j.cej.2009.03.006

Nomenclature

List of symbols

a_v	specific interfacial area ($m^2\ m^{-3}$)
c	molar concentration ($mol\ m^{-3}$)
D_l	effective liquid diffusion coefficient ($m^2\ s^{-1}$)
d_c	column diameter (m)
e	index of tray
E_A	reaction activation energy ($J\ mol^{-1}$)
ET_L	number of the tray where the liquid feed enters
ET_G	number of the tray where the gaseous feed enters
$\dot{F}$	feed molar flow ($mol\ s^{-1}$)
Ha	Hatta number
h	molar enthalpy of a stream ($J\ mol^{-1}$)
h_{liquid}	liquid level on a tray (m)
$\Delta_R H$	reaction enthalpy ($J\ mol^{-1}$)
k_G	mass-transfer coefficient in gas phase ($mol\ s\ kg^{-1}\ m^{-1}$)
k_l	mass-transfer coefficient in liquid phase ($m\ s^{-1}$)
k_V	reaction rate constant
$k_{V\infty}$	pre-exponential factor
$\dot{L}$	molar flow of the liquid ($mol\ s^{-1}$)
$\dot{N}$	specific molar flow ($mol\ m^{-2}\ s^{-1}$)
N_{ET}	number of trays in the column
N_I	number of components
N_R	number of reactions
P°	pure component saturated vapors' pressure (Pa)
P_i	partial pressure of the i-th component (Pa)
P_{total}	total pressure in the system (Pa)
$\dot{Q}_R$	reaction heat ($J\ s^{-1}$)
$\dot{Q}_d$	heat input ($J\ s^{-1}$)
$\mathbb{R}$	reflux ratio
T	temperature (K)
$\dot{V}$	gas molar flow ($mol\ s^{-1}$)
V_R	reaction mixture volume on a tray (m^3)
x	liquid molar fraction
y	gas molar fraction
z	distance in the film (m)

Greek symbols

γ	activity coefficient
δ	film thickness (m)
ν	stoichiometric coefficient
$\dot{\xi}_V$	reaction rate ($mol\ m^{-3}\ s^{-1}$)

Superscripts

*	interface
$^\circ$	pure component
^{G}	gas phase
^{L}	liquid phase
^{T}	actual temperature

Subscripts

cond	condenser
D	distillate
e	index of tray
f	liquid film
F	feed
i	index of component
j	index of reaction
l	liquid phase
L	liquid stream
LD	liquid reflux stream
V	vapor stream
z	position in the liquid film

els, according to the assumptions and simplifications applied were developed [8]. Practically all papers dealing with RD are focused on heterogeneously catalyzed reactions ([9–15], etc.). A specific case of RD represents reactions proceeding homogeneously in the liquid phase; e.g., esterification catalyzed by mineral acids [16], or consecutive reactions like epoxidation [17–19].

Description of multicomponent mass-transfer through the liquid film can be carried out by various models. Taylor and Krishna [8] and Krishna and Wesselingh [20] strongly advised the use of the Maxwell–Stefan approach (MS). There is a lot of papers dealing with heterogeneously catalyzed RD (e.g., no reaction in the liquid film), and only a few papers considering homogeneous RD [21] using the MS approach. Another possibility of describing mass-transfer accompanied by chemical reaction is the use of a simplified form of the multicomponent Fick's law. This approach is used to model G/L reactors or reactive absorption [22,23]. Frank et al. [24] analyzed mass-transfer with reversible chemical reaction in liquid film using both the MS approach and the simplified Fick's law. They analyzed only a film with fixed boundary conditions assumed for all reactants. According to their analysis, the MS approach provides more exact results than the simplified Fick's law, especially when strong concentration non-idealities occur in the liquid phase. On the other hand, the authors claim numerical problems accompanying fast reaction. Kenig et al. [25] utilized the analytical solution of the mass-transfer-and-reaction problem; however, linearization of the reaction source term is necessary. The use of the generalized multicomponent Fick's law is much simpler and it requires fewer parameters. For very fast chemical reactions, the concentration profile of a component along the liquid film can be very steep [22] and appropriate discretization along the film coordinate has to be applied to solve the governing equations numerically. The adaptive computational grid is time-saving, reducing the overall number of equations and providing higher robustness of the solution, especially in case of strong interaction between the reaction and mass-transfer occurring in the liquid film. All these facts point to the solution algorithm robustness if very fast chemical reactions proceed. Stability of the solution is important in the simulation of an RD column in which the mass-transfer and chemical reaction rates are significantly changing from one tray to another, especially during the design calculations, when no information on the temperature and concentration profiles are available and the hardware parameters are unknown.

This paper represents a continuity with a previous one concerning reaction in a CSTR [26]. Non-equilibrium steady state model of an RD column with very fast homogeneous reversible reaction proceeding in the liquid phase is presented, with the simplified multicomponent Fick's law describing the mass-transfer and chemical reaction at the *V–L* interface. Such reaction systems appear in alkylations or epoxidations [17–19]. In the paper, the presented algorithm for model equations solution allows simulation of the RD column even with fast chemical reactions. This can be useful mainly in case of the column performance optimization or in safety analysis, when stability and robustness of the solution are required not to fail when the column parameters and performance conditions are changed in a wide range. Such situation can arise when HAZOP analysis is accomplished using a mathematical model to find consequences of deviations from normal operation point generated by HAZOP [7]. In such cases, the lower accuracy of the simplified Fick's law compared to the MS approach is overcome. As Levenspiel wrote, a $10 model is sufficient [27].

To test the proposed algorithm, it was necessary to choose the physical and chemical properties of the vapor and liquid phases (densities, molar heat capacities, heats of vaporization, etc.) and to describe the vapor–liquid equilibrium. For this purpose, the model mixture consisting of four real components (ethanol, water, acetic acid, and ethyl acetate) was chosen. The goal was not the simulation

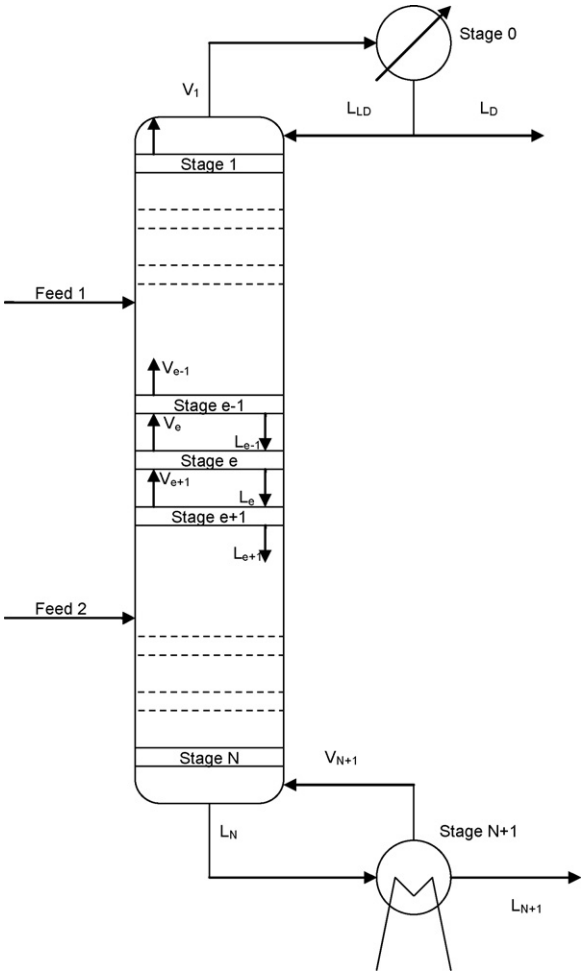

Fig. 1. Scheme of a reactive-distillation column.

and design of a real esterification process, therefore, the kinetic data used are not real.

2. Mathematical model

Mathematical model of an RD column (unit schematically drawn in Fig. 1), presented in the following text, is valid under the following assumptions:

- two-film theory,
- perfect mixing of the bulk phases,
- mass and heat transfer resistance located only in the films,
- simplified multicomponent Fick's law,
- ideal behavior of the gas phase and non-ideal behavior of the liquid phase,
- reaction taking place only in the liquid phase (both liquid film and bulk liquid),
- reboiler and condenser modeled as equilibrium,
- equilibrium between the gas and liquid phase at the *V*–*L* interface,
- constant overall pressure in the system,
- steady state,
- both phases having the same temperature.

3. Film model equations

Comparison of simplified approach using the Fick's law with effective diffusion coefficients applying the Maxwell–Stefan approach was discussed in the paper by Frank et al. [24]. Their

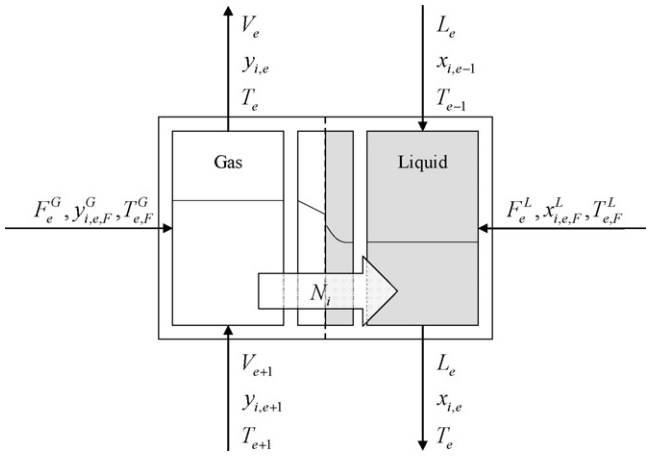

Fig. 2. Model conception of non-equilibrium reactive stage.

assumptions were

- ideal liquid and gaseous phase and
- fixed boundary conditions with zero concentration of gaseous reactant in bulk liquid and non-volatile liquid reactant, product and solvent.

Their conclusions are

- MS describes film behavior (e.g., concentration and flux profiles in the liquid film) more precisely than the Fick's law with effective diffusion coefficient and
- there could be some numerical problems solving the model equations, especially for fast chemical reactions.

However, solution of the film model equations using the MS approach with chemical reaction in the liquid film was considered. For very slow reactions, the production/consumption rates of components involved in the chemical reaction in liquid film were negligible with respect to bulk liquid rates and therefore the film reaction can be neglected and the liquid film can be treated without chemical reaction (very slow and slow regimes according to the analysis of Doraiswamy and Sharma [28]). For fast and very fast chemical reactions, some problems with the numerical solution using MS (and especially when assuming non-idealities in the liquid phase) were observed. This was the reason for using the simplified approach given by the Fick's law with effective diffusion coefficients.

Applying the assumptions mentioned in Section 2, the reaction–diffusion equation describing the reaction and diffusion processes in the liquid film for the *i*-th component in the mixture on the *e*-th tray (Fig. 2) could be written in the form:

$$D_{l,i}\left(\frac{d^2c_{f,i}}{dz^2}\right) = -\sum_{j=1}^{N_R}\nu_{i,j}\dot{\xi}_{V,z,j} \tag{1}$$

where $D_{l,j}$ is the diffusion coefficient of species *i* in the liquid phase, $c_{f,i}$ is the concentration of species *i* in the liquid film, *z* is the distance in the liquid film, $\nu_{i,j}$ the stoichiometric coefficient of species *i* in the reaction *j* and $\dot{\xi}_{V,z,j}$ stands for the reaction rate of reaction *j* in the distance *z* from the interface, with boundary conditions (BCs):

$$\begin{aligned} z &= 0, \quad c_{f,i} = c_{f,i}^{*} \\ z &= \delta, \quad c_{f,i} = c_{l,i} \end{aligned} \tag{2}$$

Solution of Eq. (1) with BCs (2) gives concentration profiles of all components in the liquid film, and of the governing mass fluxes

across the *V–L* interface (3) and from the liquid film to bulk liquid (4). These fluxes are necessary for completing the material balances in the bulk phases:

$$(\dot{N}_i)_{z=0} = -D_{l,i}\left(\frac{dc_{f,i}}{dz}\right)_{z=0} = k_{G,i}(\gamma_i P_i^{\circ} x_{f,i}^{*} - P_i) \tag{3}$$

$$(\dot{N}_i)_{z=\delta} = -D_{l,i}\left(\frac{dc_{f,i}}{dz}\right)_{z=\delta} \tag{4}$$

where $\dot{N}_i$ is the molar flux of component i, $k_{G,i}$ the mass-transfer coefficient in the gas phase, γ_i the activity coefficient of species i, P_i° the saturated vapors' pressure of pure component i, $x_{f,i}^{*}$ is the molar fraction of component i in the liquid film at the interface and P_i is the partial pressure of component i in the gas phase.

4. Column model

Material balances of the i-th component on the e-th tray can be written as follows:

- in bulk liquid:

$$\dot{F}_e^L x_{i,e,F}^L + \dot{L}_{e-1}x_{i,e-1} + V_{R,e}\sum_{j=1}^{N_R}\nu_{i,j}\dot{\xi}_{V,j,e} + V_{R,e}a_v(\dot{N}_i)_{z=\delta} - \dot{L}_e x_{i,e} = 0 \tag{5}$$

  where $\dot{F}_e^L$ is the molar flow of the liquid feed on the e-th tray, $x_{i,e,F}^L$ is the component i molar fraction in the liquid feed entering the e-th tray, $\dot{L}_e$ the molar flow of the liquid leaving the e-th tray, $V_{R,e}$ the volume of the liquid holdup on tray e, $\dot{\xi}_{V,j,e}$ stands for the reaction rate of reaction j and a_v is the specific interface area.
- in bulk gas:

$$\dot{F}_e^G y_{i,e,F}^G + \dot{V}_{e+1}y_{i,e+1} - V_{R,e}a_v(\dot{N}_i)_{z=0} - \dot{V}_e y_{i,e} = 0 \tag{6}$$

  where $\dot{F}_e^G$ is the gaseous feed molar flow entering tray e, $y_{i,e,F}^G$ is the component i molar fraction in the gaseous feed entering tray e, and $\dot{V}_e$ the molar flow of the vapor leaving the e-th tray.

Tray enthalpy balance (assumption of equal temperature of all phases and film, reference state for enthalpy calculation is pure component in the liquid phase at the reference temperature (273.15 K)):

$$\dot{F}_e^G h_{F,e}^G + \dot{F}_e^L h_{F,e}^L + \dot{Q}_{R,e} + \dot{Q}_{d,e} + \dot{V}_{e+1}h_{V,e+1} + \dot{L}_{e-1}h_{L,e-1} - \dot{V}_e h_{V,e} - \dot{L}_e h_{L,e} = 0 \tag{7}$$

with $h_{F,e}^G$ standing for the enthalpy of the gaseous feed entering tray e, $h_{F,e}^L$ for the enthalpy of the liquid feed entering tray e, $\dot{Q}_{R,e}$ for the heat generated by chemical reactions of tray e, $\dot{Q}_{d,e}$ for the heat delivered to tray e, $h_{V,e}$ for the enthalpy of the gaseous stream leaving tray e and $h_{L,e}$ for the enthalpy of the liquid stream leaving tray e.

Heat generated by chemical reactions on the tray (the first term represents the heat generation in liquid bulk and the second the heat generation in the liquid film) is defined:

$$\dot{Q}_{R,e} = V_{R,e}\sum_{j=1}^{N_R}(-\Delta_R H_j)\dot{\xi}_{V,j,e} + V_{R,e}a_{v,e}\sum_{j=1}^{N_R}\int_0^{\delta}(-\Delta_R H_j)\dot{\xi}_{V,z,j,e}dz \tag{8}$$

where $-\Delta_R H_j$ are the enthalpy of reaction j and $\dot{\xi}_{V,z,j,e}$ are the rate of reaction j in distance z from the interface on tray e.

Vapor–liquid equilibrium at the interface (i-th component, e-th tray) is:

$$P_{total}y_{i,e}^{*} = P_{i,e}^{\circ}x_{i,e}^{*}\gamma_{i,e} \tag{9}$$

with P_{total} being the overall pressure, $y_{i,e}^{*}$ the species i molar fraction in the gas phase at the interface, and the summation equations are:

$$\sum_{i=1}^{N_I} x_{i,e} = 1 \tag{10}$$

$$\sum_{i=1}^{N_I} y_{i,e} = 1 \tag{11}$$

$$\sum_{i=1}^{N_I} x_{i,e}^{*} = 1 \tag{12}$$

4.1. Total condenser mathematical model

The condenser was considered to be in equilibrium state, assuming a perfect contact between the phases. If the reflux ratio is defined as

$$\mathbb{R} = \frac{\dot{L}_{LD}}{\dot{L}_D} \tag{13}$$

$\mathbb{R}$ is the reflux ratio, $\dot{L}_{LD}$ the molar flow of the liquid reflux stream and $\dot{L}_D$ the molar flow of the liquid distillate stream.

Then, material balance of the i-th component is in the form:

$$\dot{V}y_i = \dot{L}_D(\mathbb{R}+1)x_{D,i} \tag{14}$$

while

$$y_i = x_{D,i} \tag{15}$$

and finally, the condenser enthalpy balance is:

$$\dot{V}h_V - \dot{Q}_{cond} - \dot{L}_D(\mathbb{R}+1)h_{LD} = 0 \tag{16}$$

with $\dot{Q}_{cond}$ being the heat removed in condenser and h_{LD} the enthalpy of the liquid reflux stream.

4.2. Reboiler mathematical model

The reboiler was modeled in equilibrium state since all entering components were in the liquid phase. Material balance of the i-th component in the reboiler:

$$\dot{L}_N x_{i,N} + V_{R,N+1}\sum_{j=1}^{N_R}\nu_{i,j}\dot{\xi}_{V,j} - \dot{V}_{N+1}y_{i,N+1} - \dot{L}_{N+1}x_{i,N+1} = 0 \tag{17}$$

Enthalpy balance is expressed by Eq. (7) and the equilibrium Eq. (9), both with the tray number e substituted with N.

5. Solution algorithm

The mathematical model presented above consists of two subsystems:

- Ordinary second-order differential equations (1) describing reaction and diffusion in the liquid film with boundary conditions defined in two points (liquid film boundaries)—BVP problem.
- System of non-linear algebraic equations (NAE) comprising enthalpy balances (7) and all components' material balances in bulk liquid (5) and vapor/gas phase (6), summation equations (10)–(12), thermodynamic equilibrium (9) and condenser model (14)–(16).

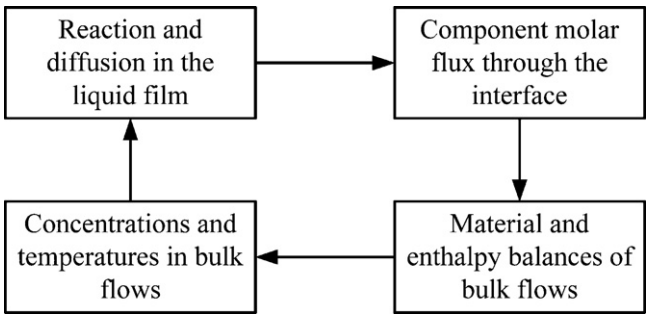

Fig. 3. Mathematical model solution structure using film model.

The proposed algorithm was built in the FORTRAN programming language using the Compaq Visual Fortran Developer Studio. The whole integral system of NAE could be solved by an appropriate solver. In this case, the algorithm proposed by Ferraris and Tronconi [29] was used. Values of calculated variables were estimated only once (at the computation start, usually values from the EQ model). Inside each iteration of the NAE solution on each tray, a system of ODE (BVP) had to be solved using actual bulk concentrations as BCs, providing mass fluxes at the vapor–liquid interface and liquid film–bulk liquid interface which are necessary for the completion and solution of material balances in bulk phases. This algorithm is schematically depicted in Fig. 3. Concentration profile in the film was estimated to be linear with the actual concentration in bulk liquid and *V–L* interface being the boundary values (see block diagram—Fig. 4).

For very fast chemical reactions, the concentration profile of a component along the liquid film can be very steep [22] and appropriate discretization along the film coordinate has to be applied to calculate the space derivations of the dependent variables (concentrations) numerically. For this reason, the algorithm proposed by Pereyra [30] and implemented in the IMSL Math library as well as in the Compaq Visual Fortran Developer Studio (the DBVPFD routine) was chosen. This algorithm automatically generates a non-uniform calculation grid for the space variable. This leads to avoiding numerical problems accompanying very fast chemical reactions between reactants entering the liquid film from the vapor phase with reactants present in the liquid phase.

6. Case study

The presented mathematical model and the proposed solution algorithm were tested using the following reaction system:

$$A + B \rightarrow R + S \quad (R1)$$

$$R + S \rightarrow A + B \quad (R2)$$

with corresponding reaction rates:

$$\dot{\xi}_{V1} = k_{V1} c_A c_B \quad (18)$$

and

$$\dot{\xi}_{V2} = k_{V2} c_R c_S \quad (19)$$

proceeding in a bubble-cap tray column, characteristics of which (number of trays, reflux ratio, reboiler heat duty, etc.) are briefly described in Table 1.

Only physical and chemical properties were modeled as for the system of acetic acid esterification with ethanol (A = acetic acid, B = ethanol, R = ethyl acetate, and S = water) and they were taken from the HYSYS database and Reid et al. [31]. To calculate activity coefficients in the liquid phase, the WILSON equation was chosen. Kinetic parameters were varied in the simulations to show the effect of very fast reaction rates on the column behavior and they are not

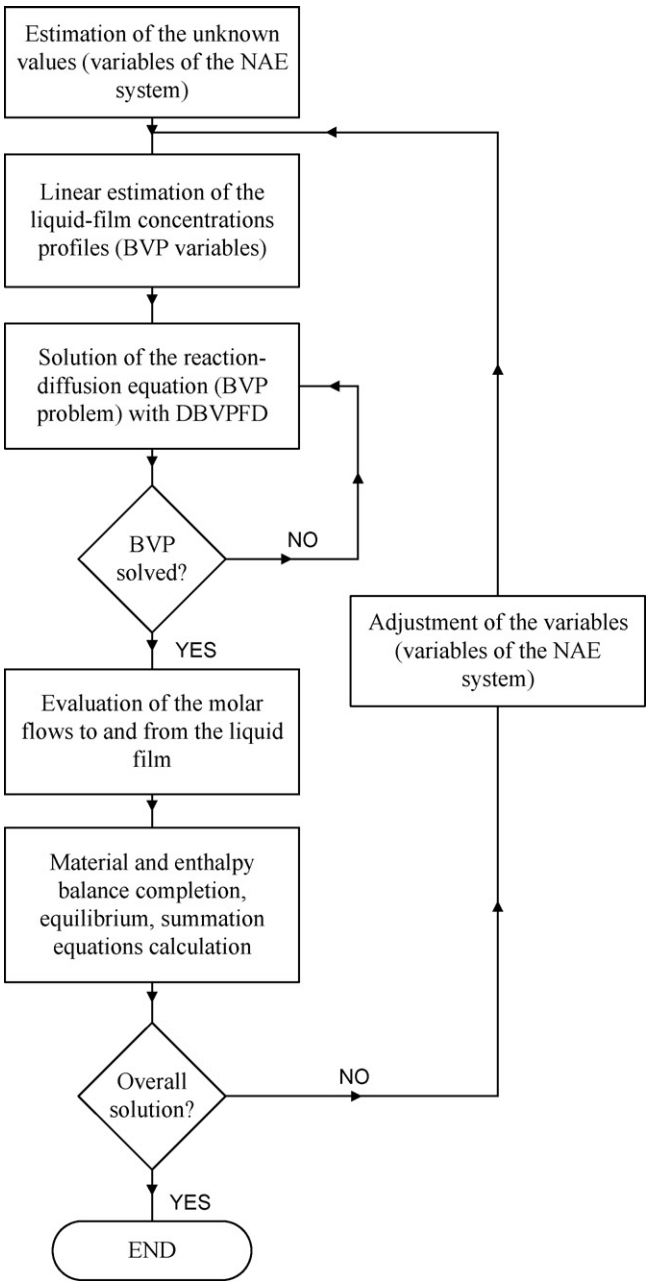

Fig. 4. Block diagram of the algorithm.

Table 1
Column characteristics.

Specific interface area	a_v (m^2 m^{-3})	240
Column diameter	d_c (m)	0.6
Number of trays	N_{ET}	20
Position of the liquid feed	ET_L	5
Position of the gaseous feed	ET_G	15
Height of the liquid on a tray	h_{liquid} (m)	0.05
Overall pressure in the column	P_{total} (Pa)	101,325
Heat delivered into the reboiler	$\dot{Q}_d$ (J s^{-1})	1.25×10^5
Reflux ratio	$\mathbb{R}$	5
Condenser temperature	T_{cond} (K)	330.5
Volume of the liquid in the reboiler	$V_{reboiler}$ (m^3)	1

Table 2
Selected kinetic parameters.

Number of components in the system	N_I	4
Number of reactions in the system	N_R	2
Reaction enthalpy	$\Delta_R H_1$ (J mol^{-1})	−4000
Reaction enthalpy	$\Delta_R H_2$ (J mol^{-1})	4000
Activation energy	E_{A1} (J mol^{-1})	5000
Activation energy	E_{A2} (J mol^{-1})	5000
Frequency (pre-exponential) factor	$k_{V\infty 1}$ (m^3 mol^{-1} s^{-1})	5.28×10^{-8}–5.28×10^{-2}
Frequency (pre-exponential) factor	$k_{V\infty 2}$ (m^3 mol^{-1} s^{-1})	1.35×10^{-8}

Table 3
Parameters of feeds.

	T (K)	Phase	$\dot{F}$ (mol s^{-1})	x_A	x_B	x_R	x_S
1	330.15	Liquid	1.1	0.98	–	–	0.02
2	352.15	Gaseous	1.1	–	0.98	–	0.02

related with any real esterification process. Temperature dependence of the reaction rate was defined by the Arrhenius equation (see Table 2).

In all simulations, the pre-exponential factor of reaction (R2) was constant. The pre-exponential factor of reaction (R1) was varied from 5.28×10^{-8} to 5.28×10^{-2} (m^3 mol^{-1} s^{-1}). Feed parameters are summarized in Table 3. Component B was fed in the gaseous phase in order to achieve intensive counter-current mass-transfer of reactants in the liquid film. Values of the specific interface area and mass-transfer coefficients were calculated from the correlations for bubble-cap tray column as published by Trambouze and Euzen [32]. Values of the liquid and vapor film thicknesses were estimated in accordance with Taylor and Krishna [33] (0.01–0.1 mm for the liquid film and 0.1–1 mm for the gaseous film). Multicomponent Wilke-Chang (liquid phase) and Fuller (gas phase) equations [31] were used to calculate the diffusion coefficients.

7. Results and discussion

To investigate the influence of parallel multicomponent mass-transfer and very fast homogeneous chemical reaction in the liquid phase on the RD column behavior, the Hatta number was used defined as

$$Ha_e^2 = \frac{\dot{\xi}_{V1,e} D_{l,B}}{k_{l,B}^2 c_{B,e}} \quad (20)$$

where k_l is the liquid-side mass-transfer coefficient. The Hatta number, defined by Eq. (20) was used only as an indicator of the reaction–diffusion conditions in the liquid film on current stage of the column. The Hatta number was evaluated on each tray with respect to the actual conditions (temperature, liquid mass-transfer coefficients and bulk liquid concentration of reactants A and B). Low Hatta number values indicate that a reaction–diffusion process in the liquid film is kinetically controlled; on the other hand, high values of the Hatta number indicate the diffusion to be the rate-controlling step.

Before proceeding with the reaction rate increase, the proposed model and algorithm were compared with the EQ model. The comparison was performed under the conditions of the lowest pre-exponential factor of reaction (R1). Temperature profiles (Fig. 5) in the column calculated by both models were very similar as well as the concentration profiles (Fig. 6).

Thus, the EQ model approach is sufficient and exact enough to simulate the processes of an RD with lower reaction rates.

After increasing the chemical reaction rates, application of the two-film theory brings significantly different results as the EQ model. This can be seen in Figs. 7 and 8.

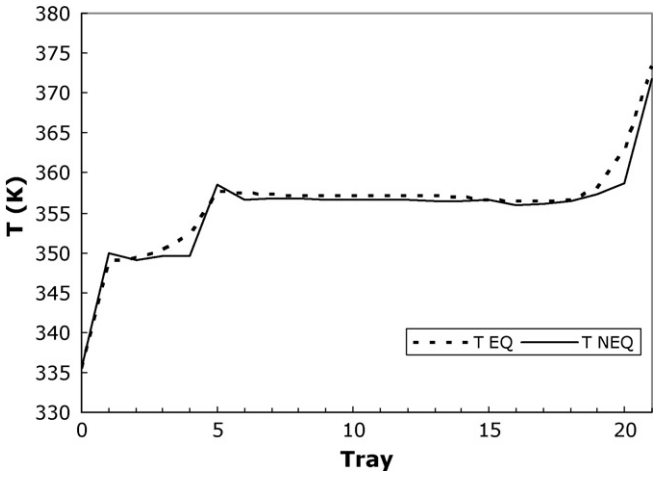

Fig. 5. Algorithm comparison with EQ—temperature profiles at the lowest pre-exponential factor ($k_{V1\infty} = 5.28 \times 10^{-8}$ m^3 mol^{-1} s^{-1}).

Different concentration profile predictions can play an important role in designing the devices for reactive separations. Different models predict also different temperature profiles in the column, which can be seen in Fig. 9. Especially on tray 15 (gaseous feed), where the temperature predicted by the NEQ model is lower than that predicted by the EQ model. This is a result of the near zero concentration of the high-boiling component A and the still low concentration of product S.

Usually, the Hatta number is calculated at a "standardized" concentration (e.g., concentration in the feed stream) of the key component and the reaction rate is evaluated under this standardized condition. In the presented paper, the Hatta number was evaluated on each tray respecting the actual conditions (temperature and concentrations of all components in the bulk liquid phase).

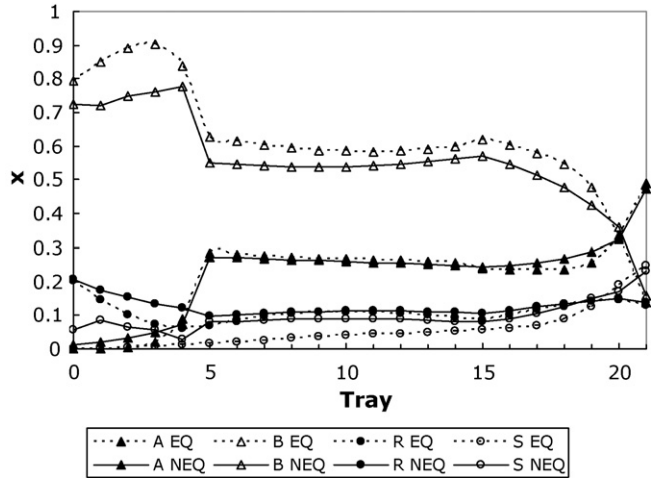

Fig. 6. Molar fractions in the bulk liquid at the lowest pre-exponential factor ($k_{V1\infty} = 5.28 \times 10^{-8}$ m^3 mol^{-1} s^{-1}).

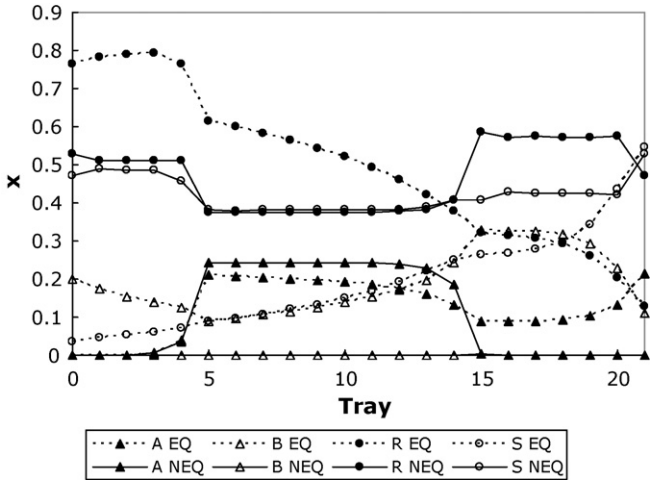

Fig. 7. Molar fractions in the bulk liquid at the highest pre-exponential factor ($k_{V1\infty} = 5.28 \times 10^{-2}$ m^3 mol^{-1} s^{-1}).

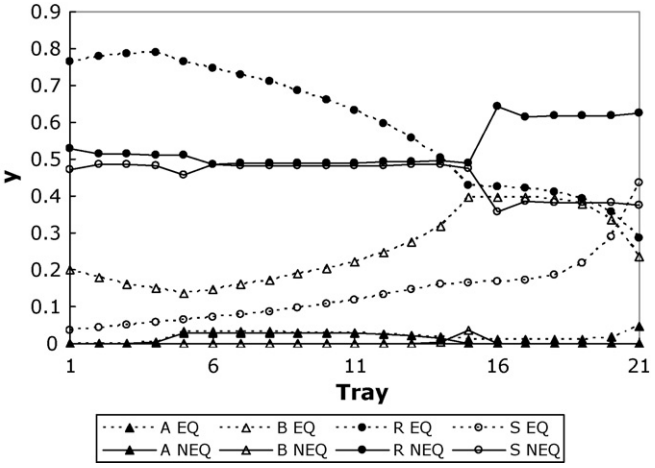

Fig. 8. Molar fractions in the bulk gas phase at the highest pre-exponential factor ($k_{V1\infty} = 5.28 \times 10^{-2}$ m^3 mol^{-1} s^{-1}).

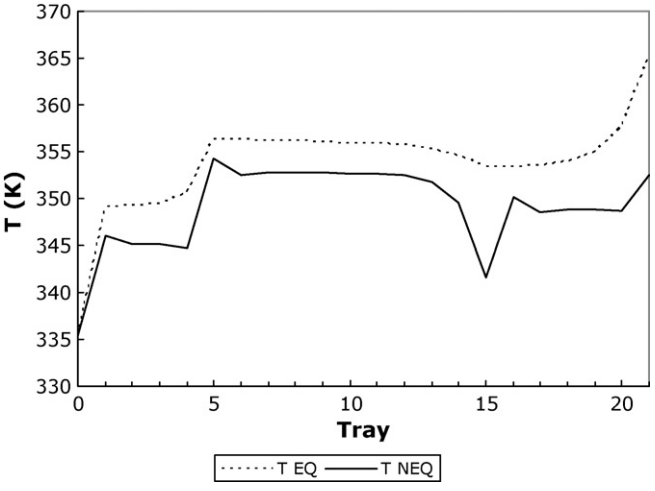

Fig. 9. Temperature profiles in the column at the highest pre-exponential factor ($k_{V1\infty} = 5.28 \times 10^{-2}$ m^3 mol^{-1} s^{-1}).

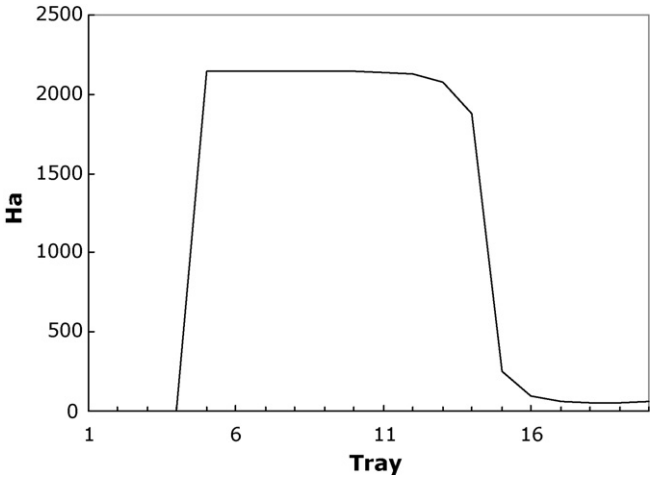

Fig. 10. Hatta number values at the highest pre-exponential factor ($k_{V1\infty} = 5.28 \times 10^{-2}$ m^3 mol^{-1} s^{-1}).

This can result in even higher values (Fig. 10) of the Hatta number. It can be seen from the figure that mass-transfer coupled with chemical reaction is very distinctive in the section between the reactants feeds. In the regime of low reaction rates (below the lower feed tray), values of the modified Hatta number were around 2.

To simulate higher mass-transfer resistance, the value of liquid film thickness was increased to the highest recommended value according to Taylor and Krishna [33]. In this case, the investigation of mass-transfer and reaction in the liquid film became more important. The number of discretization points in the film increased again in the space between the feed trays (Fig. 11). If the Maxwell–Stefan approach is used to model a reaction and diffusion, the film is usually divided into a uniformly discretized grid. Even if this grid is dense enough to obtain final results, it can be insufficient in the process of iteration (as reported by [24]). The next shortcoming of such an approach dwells in the number of equations. Number of the discretization points is usually set to a certain value even on the stages where it is not necessary.

The applied algorithm for solving the reaction–diffusion equations uses non-uniform discretization of the computational grid. This leads to a denser grid where needed (both in the film and along the column) and sparse on the trays without strong chemical reaction influence in the film (Fig. 11). The starting number of the grid points was 15. The above mentioned non-uniform discretization is

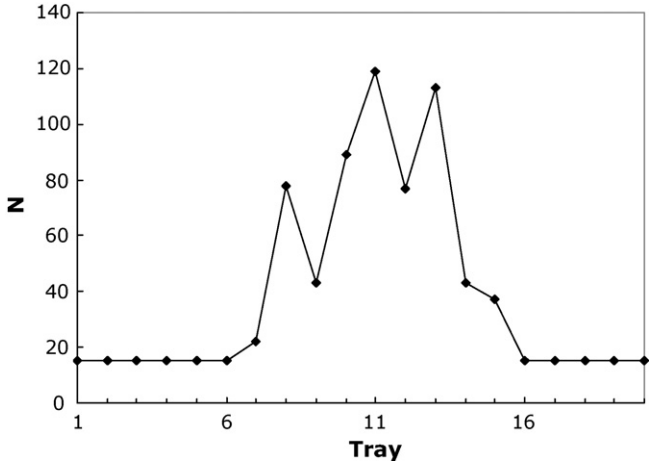

Fig. 11. Number of final discretization points in the liquid film ($k_{V1\infty} = 5.28 \times 10^{-2}$ m^3 mol^{-1} s^{-1}).

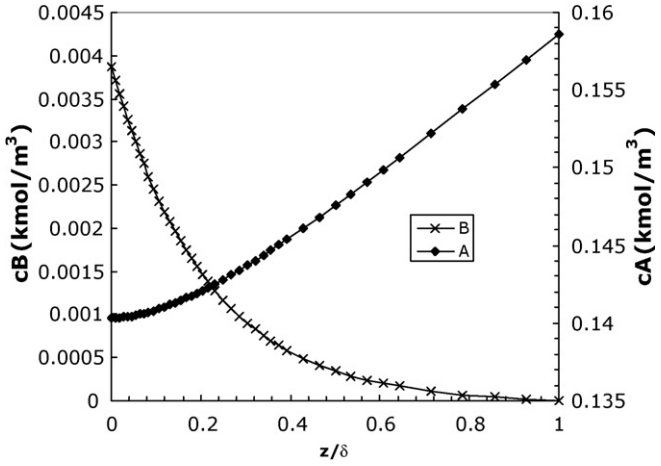

Fig. 12. Concentration profiles of the reactants in the liquid film on the 14th tray ($k_{V1\infty} = 5.28 \times 10^{-2}$ m^3 mol^{-1} s^{-1}).

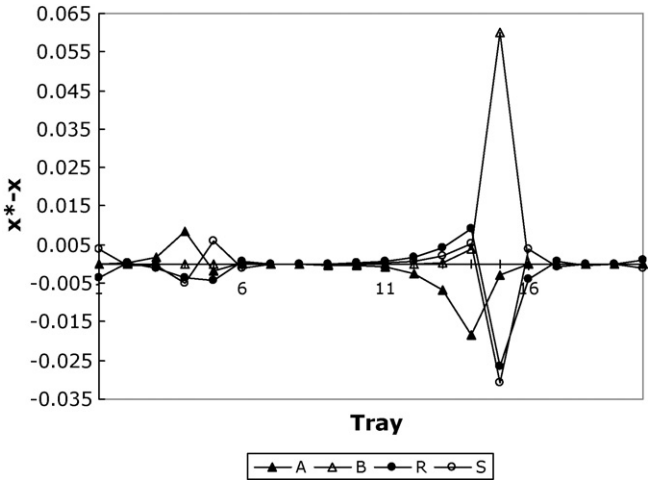

Fig. 14. Overall mass-transfer driving force across the liquid film ($k_{V1\infty} = 5.28 \times 10^{-2}$ m^3 mol^{-1} s^{-1}).

very effective (sparse computational grid in the region with linear concentration profile, dense in the areas with curved profile), as can be seen from Figs. 12 and 13.

In these figures, the concentration profiles in the liquid film on tray 14 are depicted. Due to the high reaction rate, the concentration profile of component B (fed in gaseous phase) is quite steep (Fig. 12). If the reactant was a permanent gas, the profile would be even steeper. But the reactant is present also in the bulk liquid, so the driving force is smaller. The grid density is low in the area where the concentration profiles are flat and higher where the reaction and diffusion process gets more intensive. The concentration profile of product *R* reaches a peak (Fig. 13). Since the respective reactants enter from the opposite sides of the film and diffuse against each other, the highest rate of production occurs in the place with the highest reactant concentration conjunction. Variable density of the computational grid in the liquid film leads to better stability of the solution, which is important in the case of the RD column design when the column and process parameters vary, and for the safety analysis of the RD column simulating drastic changes of the process parameters due to different technological problems.

The overall mass-transfer driving forces in the column can be seen in Fig. 14. The points represent the difference of concentrations on the boundaries of the liquid film. Positive values represent the driving forces of mass-transfer from the gaseous phase to the liquid film and vice versa. The most significant driving force is on the feed trays. Numerically, the values are relatively small because of the already mentioned presence of the reactant in the bulk liquid. The picture is only illustrative and general as the overall driving force does not respect the case of mass-transfer in both directions. It can be seen from Fig. 13 that the product passes to both the gaseous phase and the bulk liquid due to the concentration gradients.

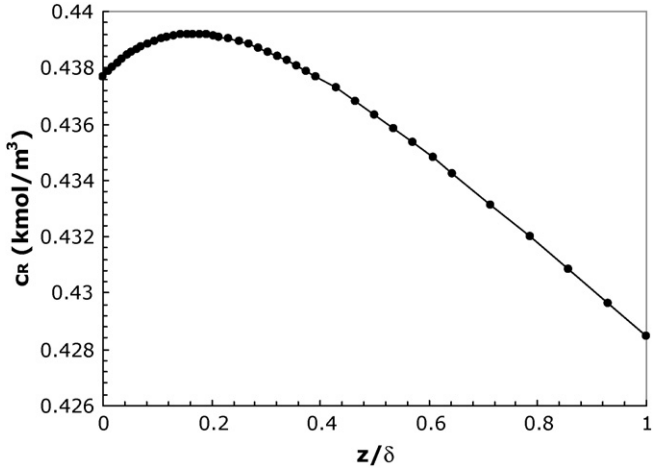

Fig. 13. Concentration profile of the product in the liquid film on the 14th tray ($k_{V1\infty} = 5.28 \times 10^{-2}$ m^3 mol^{-1} s^{-1}).

8. Conclusion

A steady-state simulation of the reactive distillation column with fast homogeneous chemical reaction in the liquid phase is presented in this paper. The non-equilibrium approach was chosen and the results were compared to those from the equilibrium model. The system is created by four components taking part in a homogeneously catalyzed reverse chemical reaction which is fast in the direct way. Chemical and physical data were modelled as for a system of acetic acid esterification with ethanol. Mass-transfer data were calculated from the empirical equations for a bubble-cap tray column. The reboiler and the condenser were modeled as equilibrium. Mass-transfer and reaction in the liquid film were described by the reaction–diffusion equation derived from the simplified multicomponent Fick's law.

Mathematical model of the column is formed of a system of non-linear algebraic equations and second-order ordinary differential equations with boundary conditions given at two points. The solution algorithm is based on a two-cycle loop, where the BVP problem is solved inside each iteration of the outer cycle. A solver using non-uniform discretization of the computational grid of the space variable was used to solve the BVP.

The developed algorithm was first tested considering the conditions with low reaction rate, thin liquid film and the results were compared to those of the EQ model. A good agreement can be stated. In the next step, the reaction rate was increased to simulate a regime limited by the diffusion in the liquid film. In order to simulate bad hydrodynamic conditions, thickness of the liquid film was increased.

To conclude, a mathematical model is presented along with the proper solvers, the algorithm is robust and simpler than the one using the Maxwell–Stefan approach. Thus, a model with less parameters was obtained. Of course, the proposed algorithm can be used to model reactive absorption processes without any significant modification of the program.

Acknowledgements

This work was supported by the Science and Technology Assistance Agency under the contract No. LPP-0181-06 and Slovak Grant Agency under the contract No. 4447/07.

References

[1] G.J. Harmsen, Reactive distillation: the front-runner of industrial process intensification—a full review of commercial applications, research, scale-up, design and operation, Chemical Engineering and Processing 46 (9) (2007) 774–780.
[2] A. Molnár, J. Markoš, Ľ. Jelemenský, Some considerations for safety analysis of chemical reactors, Transaction on IChemE, Part A: Chemical Engineering Research & Design 83 (A2) (2005) 167–176.
[3] J. Labovský, Z. Švandová, J. Markoš, Ľ. Jelemenský, Mathematical model of a chemical reactor–useful tool for its safety analysis and design, Chemical Engineering Science 62 (18–20) (2007) 4915–4919.
[4] Z. Švandová, Ľ. Jelemenský, J. Markoš, A. Molnár, Steady state analysis and dynamical simulation as a complement in the HAZOP study of chemical reactors, Transactions on IChemE, Part B: Process Safety and Environmental Protection 83 (B5) (2005) 463–471.
[5] Z. Švandová, J. Markoš, Ľ. Jelemenský, HAZOP analysis of CSTR with utilization of mathematical modeling, Chemical Papers 59 (6b) (2005) 464–468.
[6] J. Labovský, Ľ. Jelemenský, J. Markoš, Safety analysis and risk identification for tubular reactor using the HAZOP methodology, Chemical Papers 60 (6) (2006) 454–459.
[7] J. Labovský, Z. Švandová, J. Markoš, Ľ. Jelemenský, Model-based HAZOP study of a real MTBE plant, Journal of Loss Prevention in the Process Industries 20 (3) (2007) 230–237.
[8] R. Taylor, R. Krishna, Modelling reactive distillation, Chemical Engineering Science 55 (22) (2000) 5183–5229.
[9] J. Hanika, J. Kolena, Q. Smejkal, Butylacetate via reactive distillation—modelling and experiment, Chemical Engineering Science 54 (21) (1999) 5205–5209.
[10] J. Hanika, Q. Smejkal, J. Kolena, 2-Methylpropylacetate synthesis via catalytic distillation, Catalysis Today 66 (2–4) (2001) 219–223.
[11] Q. Smejkal, J. Hanika, J. Kolena, Simulation of the butyl acetate synthesis via catalytic distillation, Chemical Papers 54 (3) (2000) 165–170.
[12] Q. Smejkal, M. Soos, Comparison of computer simulation of reactive distillation using and software, Chemical Engineering and Processing 41 (5) (2002) 413–418.
[13] C. Noeres, E.Y. Kenig, A. Górak, Modelling of reactive separation processes: reactive absorption and reactive distillation, Chemical Engineering and Processing 42 (2003) 157–178.
[14] M. Kloker, E.Y. Kenig, A. Gorak, A.P. Markusse, G. Kwant, P. Moritz, Investigation of different column configurations for the ethyl acetate synthesis via reactive distillation, Chemical Engineering and Processing 43 (6) (2004) 791–801.
[15] Z. Švandová, J. Markoš, Ľ. Jelemenský, Impact of mass transfer coefficient correlations on prediction of reactive distillation column behaviour, Chemical Engineering Journal 140 (1–3) (2008) 381–390.
[16] E.Y. Kenig, H. Bader, A. Gorak, B. Bessling, T. Adrian, H. Schoenmakers, Investigation of ethyl acetate reactive distillation process, Chemical Engineering Science 56 (21–22) (2001) 6185–6193.
[17] S. Carrá, M. Morbidelli, E. Santacesaria, G. Buzzi, Synthesis of propylene oxide from propylene chlorohydrins. II. Modeling of the distillation with chemical reaction unit, Chemical Engineering Science 34 (1979) 1133–1140.
[18] S. Carrá, E. Santacesaria, M. Morbidelli, L. Cavalli, Synthesis of propylene oxide from propylene chlorohydrins. I. Kinetics aspects of the process, Chemical Engineering Science 34 (1979) 1123–1132.
[19] M. Kotora, J. Markoš, V. Čamaj, Design of a reactive distillation column for ecological decomposition of organic chloroderivatives in waste water, Chemical Engineering Science 62 (2007) 5193–5197.
[20] R. Krishna, J.A. Wesselingh, The Maxwell–Stefan approach to mass transfer, Chemical Engineering Science 52 (6) (1997) 861–911.
[21] R. Baur, R. Taylor, R. Krishna, Dynamic behaviour of reactive distillation columns described by a nonequilibrium stage model, Chemical Engineering Science 56 (6) (2001) 2085–2102.
[22] S. Carrá, M. Morbidelli, Gas–liquid reactors, in: J.J. Carberry, A. Varma (Eds.), Chemical Reaction and Reactor Engineering, Dekker, New York, 1987.
[23] J. Markoš, M. Pisu, M. Morbidelli, Modeling of gas–liquid reactors. Isothermal semibatch and continuous stirred tank reactors, Computers and Chemical Engineering 22 (4–5) (1998) 627–640.
[24] M.J.W. Frank, J.A.M. Kuipers, G.F. Versteeg, W.P.M. van Swaaij, Modelling of simultaneous mass and heat transfer with chemical reaction using the Maxwell–Stefan theory. I. Model development and isothermal study, Chemical Engineering Science 50 (10) (1995) 1645–1659.
[25] E.Y. Kenig, F. Butzmann, L. Kucka, A. Górak, Comparison of numerical and analytical solutions of a multicomponent reaction-mass-transfer problem in terms of the film model, Chemical Engineering Science 55 (8) (2000) 1483–1496.
[26] J. Sláva, Z. Švandová, J. Markoš, Modelling of reactive separations including fast chemical reactions in CSTR, Chemical Engineering Journal 139 (3) (2008) 517–522.
[27] O. Levenspiel, Modeling in chemical engineering, Chemical Engineering Science 57 (22–23) (2002) 4691–4696.
[28] L.K. Doraiswamy, M.M. Sharma, Heterogeneous reactions: analysis, examples and reactor design Fluid–Fluid–Solid Reactions, vol. 2, John Wiley and Sons, New York, 1984.
[29] G.B. Ferraris, E. Tronconi, BUNLSI—a Fortran program for solution of systems of nonlinear algebraic equations, Computers and Chemical Engineering 10 (2) (1986) 129–141.
[30] V. Pereyra, PASVA3: An Adaptive Finite-Difference Fortran Program for First Order Nonlinear, Ordinary Boundary Problems, Springer-Verlag, Berlin, 1978 (http://books.google.sk/books?id=bsSmf1NOlSgC&printsec=frontcover&source=gbs_summary_r&cad=0#PPA70,M1).
[31] R.C. Reid, J.M. Prausnitz, B.E. Poling, The Properties of Gases and Liquids, McGraw-Hill, New York, 1987.
[32] P. Trambouze, J.P. Euzen, Chemical Reactors—From Design to Operation, Institut Francais du Petrole Publications, Paris, 2002.
[33] R. Taylor, R. Krishna, Multicomponent Mass Transfer, John Wiley & Sons, Inc., New York, 1993.